Iraqi Journal of Science, 2024, Vol. 65, No. 12, pp: 7349- 7363
DOI: 10.24996/ijs.2024.65.12.44

ISSN: 0067-2904

Evaluating the Performance of Supervised Classification Algorithms in Classifying SENTINEL-2A Images on Land Cover and Land Uses of a Part of Baghdad, Iraq

Sajaa Muhsein Khazael[1], Hiba Akram Atiyah [2], Mourtadha Sarhan Sachit[1]*
[1] *Civil Engineering Department, College Engineering, University of Thi-Qar, Nasiriyah, Iraq*
[2] *Civil Engineering Department, College Engineering, Al-Iraqi University, Baghdad, Iraq*

Received: 29/5/2023 Accepted: 17/11/2023 Published: 30/12/2024

Abstract

Exploring the performance of supervised machine learning algorithms for specific classification tasks is essential to enhance the accuracy and reliability of thematic maps generated from remote sensing data, ultimately supporting informed decision-making in land use management and environmental monitoring. This paper evaluates the classification performance of supervised machine learning algorithms within a specific region of Baghdad, Iraq, primarily focusing on utilizing SENTINEL-2A imagery. The crucial initial step involves data preprocessing, meticulously executed through the application of SNAP software, setting the foundation for a comprehensive analysis of the algorithms' effectiveness. Maximum Likelihood (ML), Minimum Distance (MD), Random Forest (RF), K-Nearest Neighbor (KNN), and KD Tree KNN (KD-KNN) models are applied to produce Landuse maps of five classes. Finally, a confusion matrix is implemented to examine the classification accuracy. The results revealed the superiority of the RF classifier with an overall accuracy of 83.33%. Followed by KNN and KD-KNN with an accuracy of 80% each. Bare lands scored the highest rating in most of the applied algorithms. The reported findings raise awareness regarding selecting suitable algorithms for specific classification tasks.

Keywords: Supervised Classification, Sentinel, SNAP, RF, Baghdad.

تقييم أداء خوارزميات التصنيف الخاضعة للإشراف في تصنيف صور *SENTINEL-2A* على الغطاء الأرضي واستخدامات الأراضي لجزء من بغداد، العراق

سجى محسن خزعل [1], هبة أكرم عطيه[2], مرتضى سرحان ساجت[1]*
[1]قسم الهندسة المدنية، كلية الهندسة، جامعة ذي قار، ذي قار، العراق
[2]قسم الهندسة المدنية، كلية الهندسة، الجامعة العراقية، بغداد، العراق

الخلاصة

تتمثل أهمية استكشاف أداء خوارزميات التعلم الآلي الخاضعة للإشراف لمهام تصنيف محددة في تعزيز دقة وموثوقية الخرائط المواضيعية الناتجة عن بيانات الاستشعار عن بعد، مما يدعم في نهاية المطاف اتخاذ

*Email: murtadha-s@utq.edu.iq

القرارات المستنيرة في إدارة استخدام الأراضي والرصد البيئي. تسعى هذه الورقة إلى تقييم أداء التصنيف لخوارزميات التعلم الآلي الخاضعة للإشراف في منطقة معينة من بغداد، العراق، مع التركيز بشكل أساسي على استخدام صور SENTINEL-2A. تتضمن الخطوة الأولية الحاسمة المعالجة المسبقة للبيانات، والتي يتم تنفيذها بدقة من خلال تطبيق برنامج SNAP، مما يضع الأساس لتحليل شامل لفعالية الخوارزميات. يتم تطبيق نماذج Maximum Likelihood (ML) وMinimum Distance (MD) و Random Forest (RF) وK-Nearest Neighbor (KNN) وKD Tree KNN (KD-KNN) لإنتاج خرائط استخدام الأراضي من خمس فئات. أخيرًا، يتم تنفيذ confusion matrix لفحص دقة التصنيف. أظهرت النتائج تفوق مصنف (RF) بدقة كلية بلغت 83.33٪. تليها KNN وKD-KNN بدقة 80٪ لكل منهما. سجلت الأراضي القاحلة أعلى تصنيف في معظم الخوارزميات المطبقة. تعمل النتائج التي تم الحصول عليها على زيادة الوعي بشأن اختيار الخوارزميات المناسبة لمهام تصنيف محددة.

1. Introduction

A thematic map shows the geographic pattern of a particular subject theme in a specific geographic region. Thematic mapping is often based on image classification using manual or automated analysis [1]. Satellite images have been widely employed to classify Landuse/Landcover (LULC), which gives the ability to update maps continuously [2] and [3]. Classifying satellite images, however, is a challenging task that requires familiarity with the data's characteristics, the best classification techniques, and the local environment [4] and [5]. The correct classification of satellite images affected by snow or dust cover presents a potential difficulty in producing thematic maps.

There are two types of image classification: supervised and unsupervised; in supervised classification, training is essential because specific pixels from each class must first be recognized as training pixels (training samples) [6]. An unknown pixel can be categorized using a variety of supervised classification algorithms. It is crucial to choose the suitable classifier or decision rule because it is based on the input data type and the desired results [7], [8], and [9]. The Maximum Likelihood classifier (ML), one of the most popular classification techniques, assigns the class to the pixel with the highest likelihood [10]. Any image pixel can be classified using the Minimum Distance classifier (MD), which measures the distance between the pixel's image data and the means of the classes created from the training sets [6]. The non-parametric K-Nearest Neighbor method (KNN) classifies objects based on the nearby training samples in the feature space [11] while using a KD Tree to improve performance; the KD Tree KNN classifier (KD-KNN) should produce the same results as the slow KNN classifier. Furthermore, Random Forest (RF) is a classification and regression tree method that produces a sizable group, or forest, of classification and regression trees by randomly and iteratively sampling the data and variables [12].

LULC mapping and monitoring have been recognized as essential scientific goals in the broad literature, with the information obtained being utilized to support environmental and decision-making efforts. For instance, a study compared the classification accuracies of land cover derived from Sentinel-2 and Landsat-8 data using the Support Vector Machine (SVM) and ML approaches [13]. According to the comparison, using Sentinel-2 images resulted in the highest categorization accuracy of 84.17%. Yusof et al. conducted an interesting study to produce an accurate thematic map of land cover and the distribution of the rubber trees' growth stages in Malaysia [14]. Using the SVM technique, the scientists classified Landsat-8 OLI and Sentinel-2 pictures into seven landcover classes. According to the findings, SVM had the highest classification accuracy, with 87.22% for Sentinel-2 and 85.74 for Sentinel-1 for Landsat-8.

The area of interest (Baghdad) has been highlighted in a number of previous classification studies. Landsat TM satellite imagery produced a land use/landcover (LULC) map for the Baghdad region and nearby areas [15]. The study applied the ML method to classify the images into five classes: urban land, vegetable land, water, bare land, and uncultivated agricultural land. The results revealed that the wide coverage areas are vegetation and bare lands, and the overall classification accuracy achieved was 93%. In a separate study, [16] used the Singular Value Decomposition algorithm (SVD) and ML Classifier to detect Landcover changes in Baghdad over the past thirty years. The classification was based on five types of land cover: water body, vegetation, bare land, residential area 1, and residential area 2. The findings proved the efficiency of the SVD method, as it achieved a classification accuracy of 81%. To extract vacant land, [6] compared algorithms of MD and ML to produce a land cover for Baghdad, Iraq. For this purpose, the authors used high-resolution imagery from GeoEye-1 and classified them into five landcover categories. Both algorithms achieved similar results for the percentage of vacant lands at 15% of the total area of interest.

From the review above, there is a lack of publications that have addressed the production of thematic maps from SENTINEL-2A images in Iraq. Thus, this paper aims to evaluate supervised classification algorithms in classifying landcover classes for SENTINEL-2A images across Baghdad, Iraq. The study examined five supervised classification classifiers: ML, MD, KNN, KD-KNN, and RF. Besides, confusion matrices supported by ground truth data are applied to evaluate the accuracy of the generated thematic maps. This research highlights classification algorithms that efficiently work with SENTINEL-2A data, producing more accurate thematic maps for sustainable city development. The following sections cover the materials, methods, results, and detailed discussions.

2. Study Area

Baghdad University campus and its surroundings were chosen as a case study with an area of 22 km^2. It is located at Longitude 44º 23’ and Latitude 33º 16’ in Baghdad, Iraq. The diversified land uses and the presence of the Tigris River, which encircles the university campus, distinguish the study area, Figure 2.

Figure 2. The geographical location of the study area.

3. Materials and Methods

The proposed methodology includes three main steps, Figure 1. After defining the area of interest, the necessary remote sensing data was first collected. Data pre-processing was performed, and then five supervised machine learning algorithms were applied to generate thematic maps. Finally, predictions were evaluated according to ground truth data.

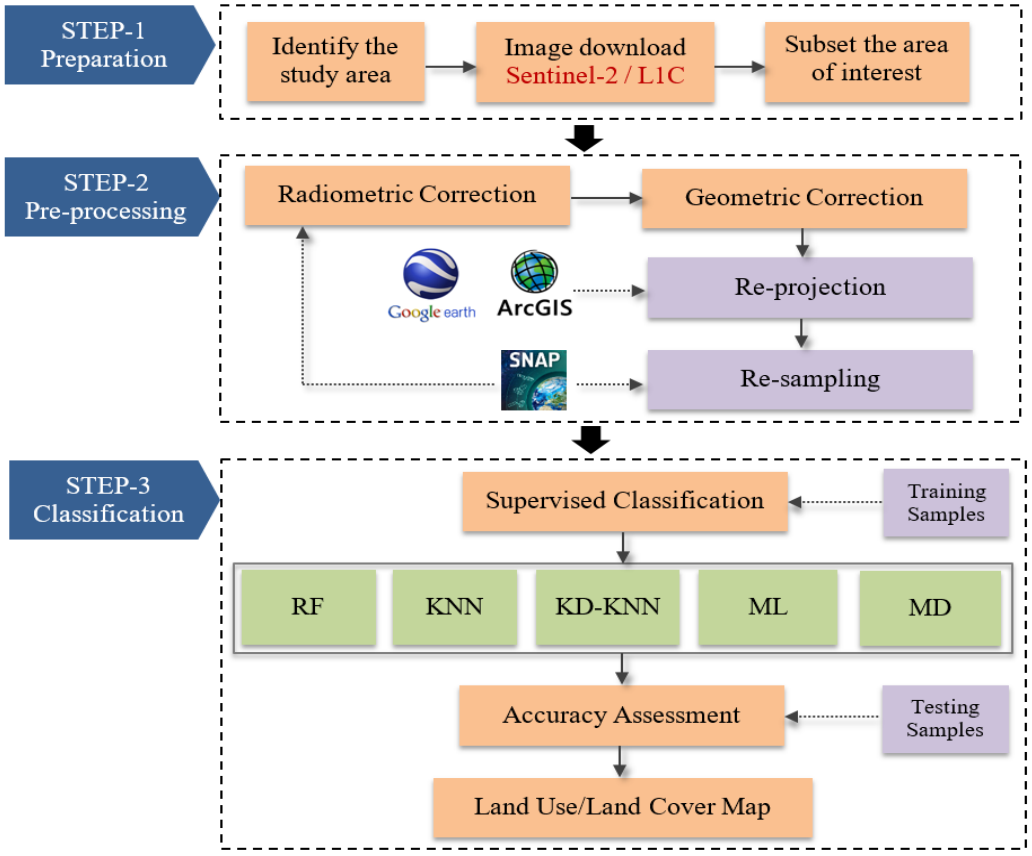

Figure 1. The methodology workflow of this study.

3.1. Data and Software

The SENTINEL-2A image was downloaded from the European Space Agency website (https://dataspace.copernicus.eu/) and served as this study's remote sensing data source. The specific characteristics of the image are listed in Table 1. Three key software were used for pre-processing and data classification: SNAP, ArcGIS, and Google Earth. SNAP, which stands for Sentinel Application Platform, is a free software of three Sentinel Toolboxes developed by the European Space Agency (ESA) for scientifically exploiting Sentinel missions [17]. Supervised image classification, radiometric image adjustment, and image subset were all accomplished with the help of SNAP. ArcGIS, on the other hand, is a geographic information system (GIS) software created by the Environmental Systems Research Institute (Esri) [18]. It was applied to execute the geometry correction in the image-to-GCPs method. Google Earth, launched by Google, is a computer program that displays a 3D representation of the Earth with many tools for measuring dimensions and coordinates, mainly based on satellite images. Google Earth was used to get the coordinates of GCPs for the validation process. Using the SNAP tool "Specify product subset," the focus from the entire image was narrowed. From the resulting B4: R, B3: G, and B2: B bands, an RGB image was subsequently exported.

Table 1. The image characteristics.

Product name	SENTINEL-2A_MSIL1C
Area of interest	Baghdad, Iraq
Product time	09-March-2021
Coordinate reference system	WGS84/UTM zone 38N
Spectral resolution	13 bands
Spatial resolution	10 m (B2, B3, B4 and B8) 20 m (B5, B6, B7, B8a, B11 and B12) 60 m (B1, B9 and B10)
Radiometric resolution	12-bit

3.2. Data Pre-processing

Pre-processing is a technique to minimize errors prior to image analysis, where the most essential pre-processing steps are radiometric correction, geometric correction, and resampling.

3.2.1. Radiometric correction

Radiometric correction can improve the relationship between the radiant flux leaving a surface and the radiant flux measured by a sensor [19]. Since digital sensors record electromagnetic radiation strength from each point seen on the Earth's surface as a Digital Number (DN) for each spectral band, the precise range of DN a sensor uses is determined by its radiometric resolution [16]. To overcome the discrepancies in sunlighting geometry, it is essential to normalize the image pixel values, where SNAS software was utilized to perform the radiometric correction: Calibration, Raster, and Radiometric.

3.2.2. Geometric Correction

Geometric correction, or rectifications, transforms image data into a map's scale and projection properties. Accurate geometric correction of the satellite imagery is required to perform precise image fusion [20]. The current paper used the image-to-GCPs method to rectify the image. In Equation (1), five ground control points (GCPs) in suitable locations were selected to execute a first-order polynomial transformation, Figure 3. The coordinates of GCPs were extracted from Google Earth, and the image rectification process was conducted using the ArcGIS software.

$$n = \frac{(t+1)(t+2)}{2} \qquad (1)$$

Where n is the minimum number of GCPs needed to calculate a transformation, t refers to the transformation order. Accordingly, the minimum number of GCPs needed for a first-order transformation is 3.

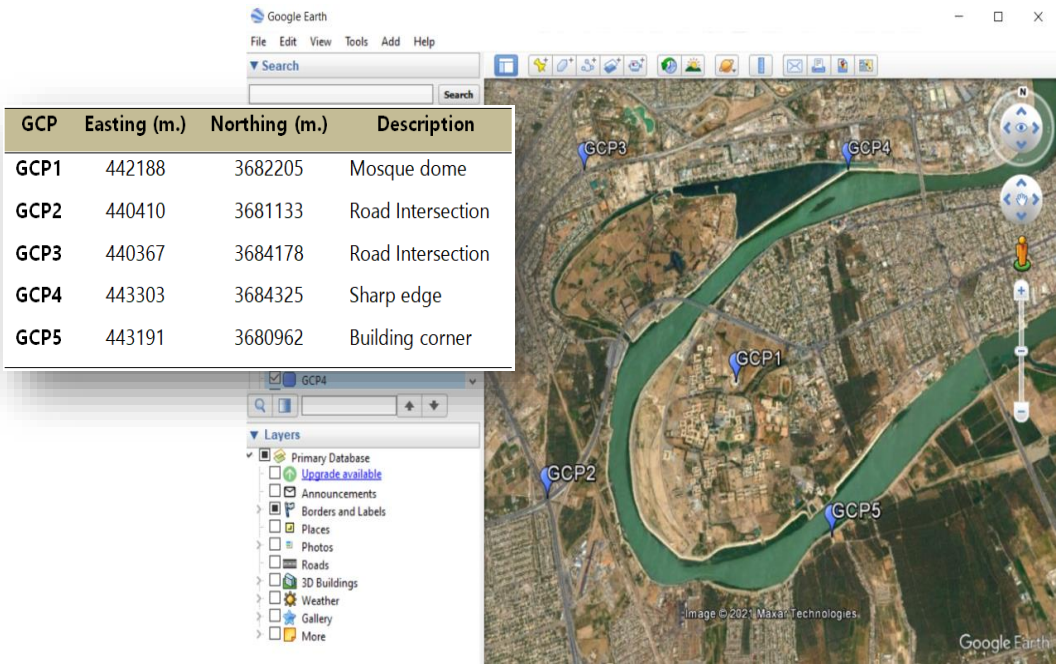

GCP	Easting (m.)	Northing (m.)	Description
GCP1	442188	3682205	Mosque dome
GCP2	440410	3681133	Road Intersection
GCP3	440367	3684178	Road Intersection
GCP4	443303	3684325	Sharp edge
GCP5	443191	3680962	Building corner

Figure 3. The locations and coordinates of the GCPs employed in the geometry correction.

3.2.3. Re-sampling

Resampling is crucial for ensuring that each band has the same resolution and number of pixels. The following processing settings were used to complete the current study's resampling task: 10 m output spatial resolution, nearest up-sampling method, and mean down-sampling method.

3.3. Image Classification

3.3.1. Training Samples

The primary goal of the training data set is to feed the classifiers with enough information to categorize the image [14] correctly. The image classification algorithm employs the training samples to identify the landcover classes in the entire image. The training samples should be homogeneous and diverse enough to produce accurate statistics [21]. The work identified five land cover classes: bare land, vegetation, buildings, roads, and water bodies. The training samples were collected using the on-screen selection method, Figure 4. Besides, the rule-of-thumb, Equation (2), was applied to calculate the minimum number of training pixels required.

$$p = 10 * n * c \qquad (2)$$

Where p is the minimum number of training pixels required, n is the number of bands, and c denotes the number of classes. For n=3 bands (B2, B3, and B4) and five classes, 30 pixels were defined for each class; thus, the total number of pixels was 150.

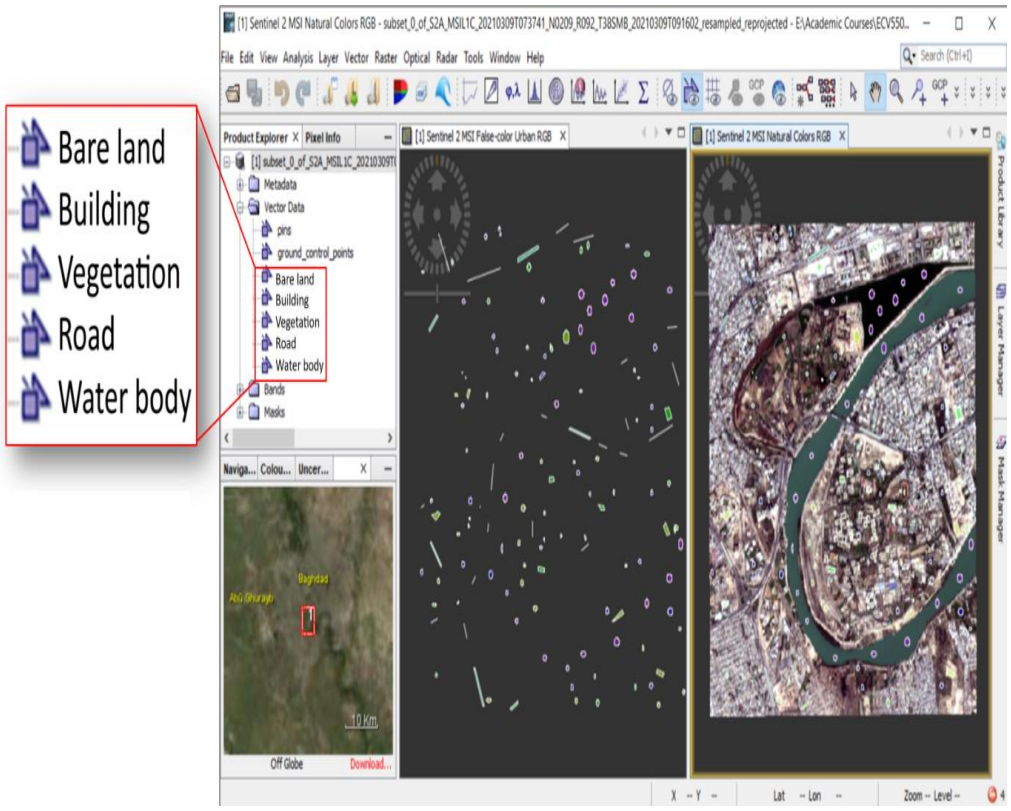

Figure 4. The training samples used the on-screen selection method via SNAP.

3.3.2. Supervised Classification Algorithms

Five distinct supervised classification algorithms were employed, one by one, with identical training samples. These methods are ML, MD, KNN, KD-KNN (KD-KNN), and RF.

One well-known supervised algorithm is ML classification. It assumes the data was usually distributed and considers the variance and covariance within the class distributions. ML could produce superior results if a dataset is normally distributed to other well-known parametric classifiers [13]. However, in ML, For data with a non-normal distribution, high accuracy values may not be obtained [22].

MD was utilized to classify RS imagery into different categories. In the MD classifier, one must first determine each class's centroid or average value and then compute the Euclidean distance between the centroid and the unknown value of the image pixel [23]. Pixels can be classified into appropriate groups using the smallest distance between them. This classifier's implementation is computationally light and intuitive [24].

The KNN classifier, a non-parametric approach, has been applied in statistical applications since the early 1970s [25]. Fundamentally, KNN identifies a set of k samples close to unknown samples in the calibration dataset. By averaging the responses to these k sets, the label (class) of the undefined samples' class features of the k nearest neighbor [26] can be inferred. As a result, k is crucial to KNN performance, serving as the classifier's primary tuning parameter. Although the KD-KNN classifier was intended to outperform the slower KNN classifier, it should still be able to achieve the same results.

RF is a powerful and widely used model for satellite image classification due to its simplicity, flexibility, and accuracy [27]. RF classifier employs a number of decision trees trained on random samples of the data and features. Each tree's output was added to the others to form the final result. The approach helps reduce overfitting and may suggest the most crucial features [28].

4. Result and Discussion

The different classification algorithms' applications resulted in thematic maps representing the land cover of the area of interest, Figure 5. The thematic maps included five classes: blue refers to water bodies, green to vegetation, red to buildings, yellow to bare lands, and grey to roads. The proportions and areas of each class differed among the five applied algorithms, as indicated in Table 2. The bare land class achieved the highest areas in most of the adopted classification methods. The buildings class reached the highest area of 6.30 km^2 in the ML classifier, while it was the lowest at 3.9 km^2 when applying the MD classifier.

On the other hand, the road category witnessed a remarkable increase in the area, achieving 7.43 Km^2, after the values were close to the rest of the algorithms. In addition, the vegetation and water body classes were relatively equal in the area among all the adopted classification algorithms. Figure 6 presents a comparison of the different landcover classes' areas across all of the algorithms that were taken into consideration.

Table 2. Percentages and regions of each class among the algorithms used

Class	Color	RF		KNN		KD-KNN		ML		MD	
		(%)	Area (Km^2)	(%)	Area (Km^2)	(%)	Area (Km^2)	(%)	Area (Km^2)	(%)	Area (Km^2)
Bare land		32.5	7.17	30.6	6.75	30.6	6.75	17.5	3.87	36.5	8.05
Building		21.7	4.80	22.4	4.94	22.4	4.94	28.5	6.30	3.9	0.86
Vegetation		16.5	3.65	15.8	3.50	15.8	3.50	24.6	5.43	13.8	3.05
Road		16.7	3.70	19.0	4.20	19.0	4.20	19.4	4.28	33.6	7.43
Water Body		12.6	2.78	12.2	2.69	12.2	2.69	10.0	2.20	12.2	2.70
Sum		100	22.09	100	22.09	100	22.09	100	22.09	100	22.09

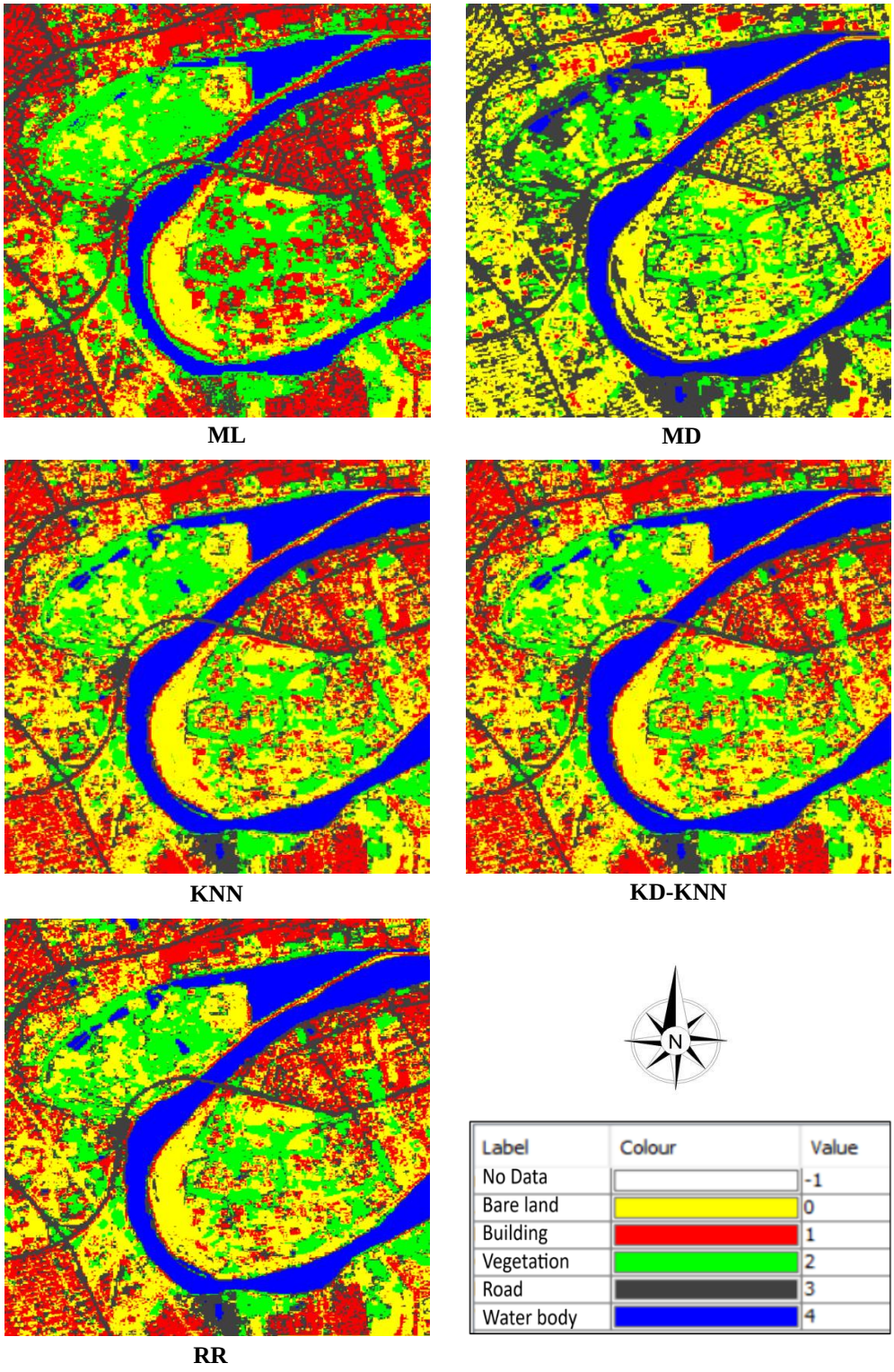

Figure 5. Thematic maps of the study area according to different classification algorithms

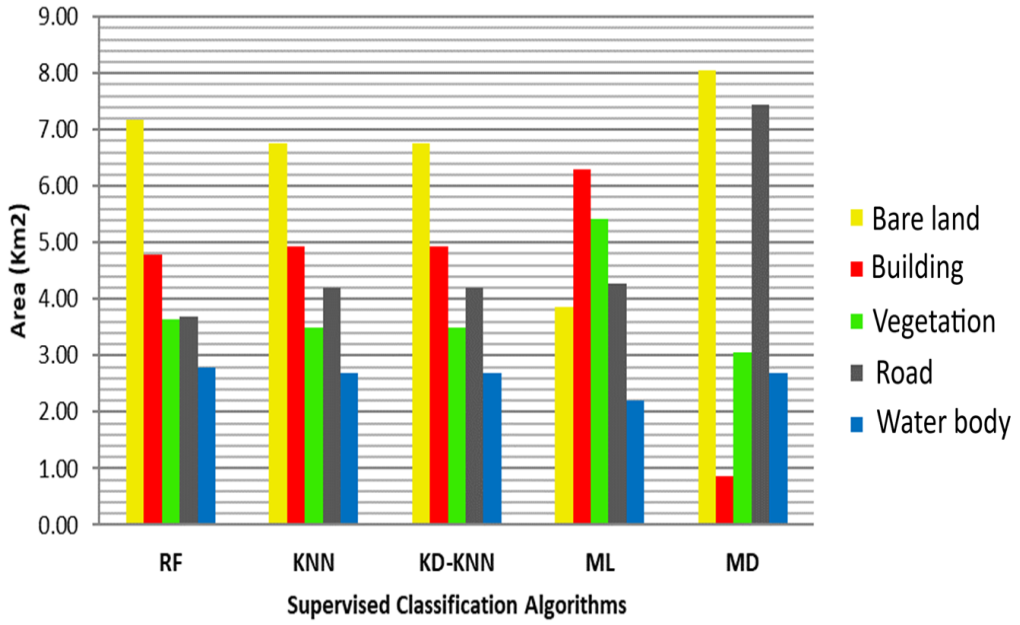

Figure 6. Variation in the area of each class across different classification algorithms

4.1. Accuracy Assessment

The accuracy of the classified map is a standard approach for validating land cover products. It compares the classified image to another source considered accurate or ground truth data [13]. Ground truth data can be obtained in the field or extracted by interpreting high-resolution images, existing classified imagery, or GIS data layers. The most common method for evaluating the accuracy of a classified map is to generate a set of random points from the ground truth data and compare them to the classified data in a confusion matrix. The confusion matrices can be used to determine the correctness of the user and the producer [14]. In this regard, 30 testing samples were randomly selected on the five classified maps, Figure 7. Then, the testing samples were compared on high-resolution images via Google Earth. Tables 3, 4, 5, 6, and 7 illustrate the confusion matrix results for the five applied algorithms. The accuracy assessment results show that the RF algorithm achieved the highest classification accuracy of 83.33%, while the lowest accuracy was 63.33 % for the MD algorithm, Figure 8.

Table 3. Confusion matrix results for the RF algorithm.

Class	Bare land	Building	Vegetation	Road	Water Body	Total Row (user)
Bare land	8	0	2	0	0	10
Building	0	6	0	1	0	7
Vegetation	0	0	2	0	0	2
Road	0	1	1	5	0	7
Water Body	0	0	0	0	4	4
Total Column (producer)	8	7	5	6	4	30
Producer's accuracy (%)	100.00	85.71	40.00	83.33	100.00	
User's accuracy (%)	80.00	85.71	100.00	71.43	100.00	
Overall accuracy			**83.33**			

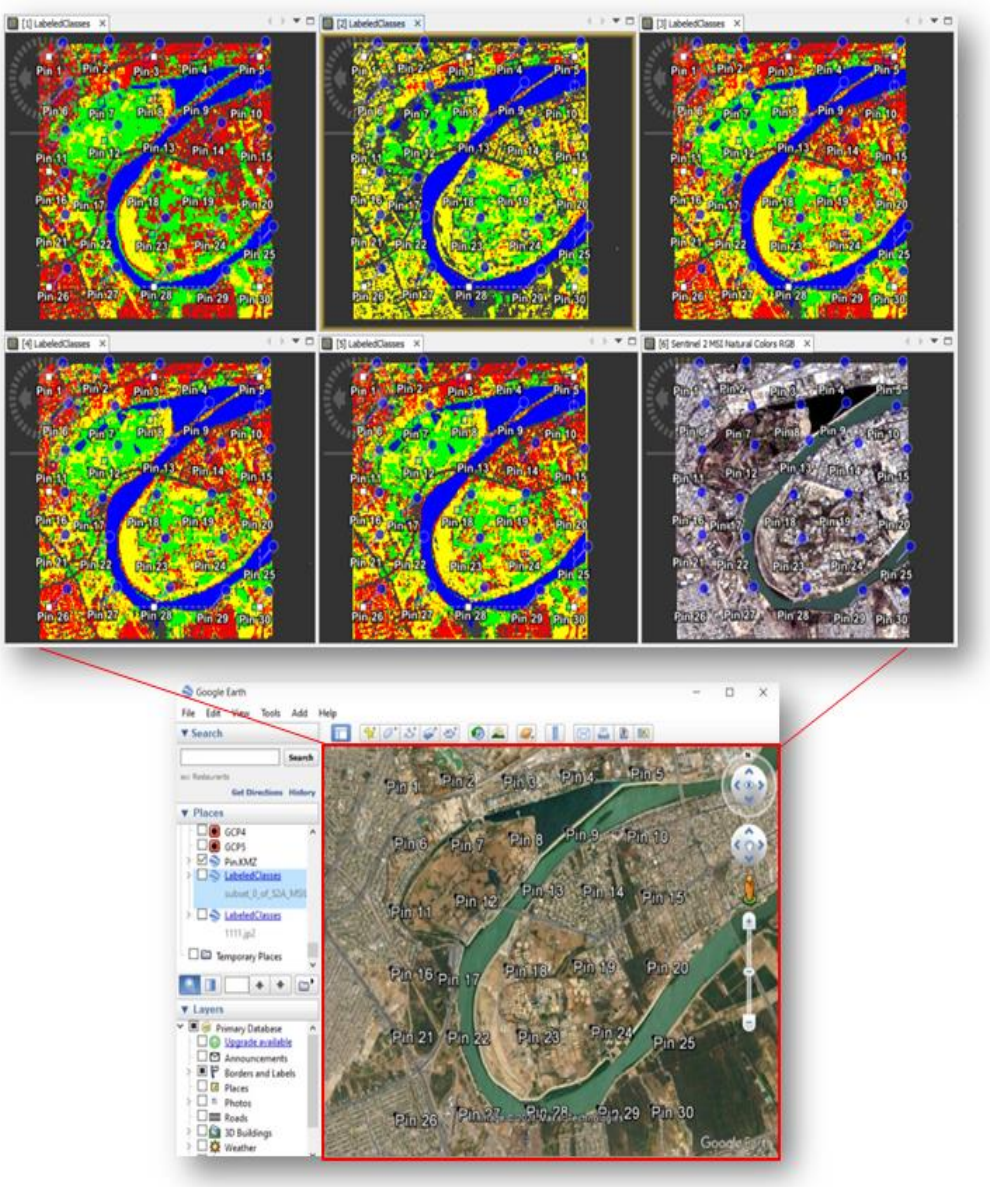

Figure 7. Locations of test samples and their counterparts on Google Earth imagery

Table 4. Confusion matrix results for the KNN algorithm

Class	Bare land	Building	Vegetation	Road	Water Body	Total Row (user)
Bare land	6	1	2	0	0	9
Building	2	6	0	1	0	9
Vegetation	0	0	3	0	0	3
Road	0	0	0	5	0	5
Water Body	0	0	0	0	4	4
Total Column (producer)	8	7	5	6	4	30
Producer's accuracy (%)	75.00	85.71	60.00	83.33	100.00	
User's accuracy (%)	66.67	66.67	100.00	100.00	100.00	
Overall accuracy			**80.00**			

Table 5. Confusion matrix results for the KD-KNN algorithm

Class	Bare land	Building	Vegetation	Road	Water Body	Total Row (user)
Bare land	6	1	2	0	0	9
Building	2	6	0	1	0	9
Vegetation	0	0	3	0	0	3
Road	0	0	0	5	0	5
Water Body	0	0	0	0	4	4
Total Column (producer)	8	7	5	6	4	30
Producer's accuracy (%)	75.00	85.71	60.00	83.33	100.00	
User's accuracy (%)	66.67	66.67	100.00	100.00	100.00	
Overall accuracy			**80.00**			

Table 6. Confusion matrix results for the ML algorithm

Class	Bare land	Building	Vegetation	Road	Water Body	Total Row (user)
Bare land	7	0	0	0	0	7
Building	0	6	0	3	0	9
Vegetation	1	0	5	1	2	9
Road	0	1	0	2	0	3
Water Body	0	0	0	0	2	2
Total Column (producer)	8	7	5	6	4	30
Producer's accuracy (%)	87.5	85.7	100.0	33.3	50.0	
User's accuracy (%)	100.0	66.7	55.6	66.7	100.0	
Overall accuracy			**73.33**			

Table 7. Confusion matrix results for the MD algorithm

Class	Bare land	Building	Vegetation	Road	Water Body	Total Row (user)
Bare land	7	5	0	1	0	13
Building	1	1	0	0	0	2
Vegetation	0	0	2	0	0	2
Road	0	1	3	5	0	9
Water Body	0	0	0	0	4	4
Total Column (producer)	8	7	5	6	4	30
Producer's accuracy (%)	87.50	14.29	40.00	83.33	100.00	
User's accuracy (%)	53.85	50.00	100.00	55.56	100.00	
Overall accuracy			**63.33**			

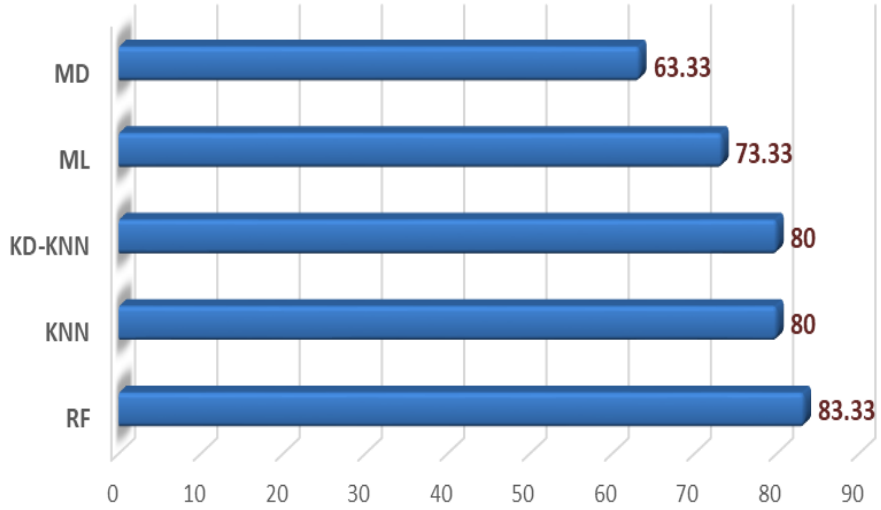

Figure 8. The overall accuracy of the algorithms is considered

4.2 Visual Verification

Visual verification of the final RF-produced thematic map was performed for more confidence, Figure 9. From the pictorial comparisons, it can be seen that there is a great agreement between the land cover category and the ground reality.

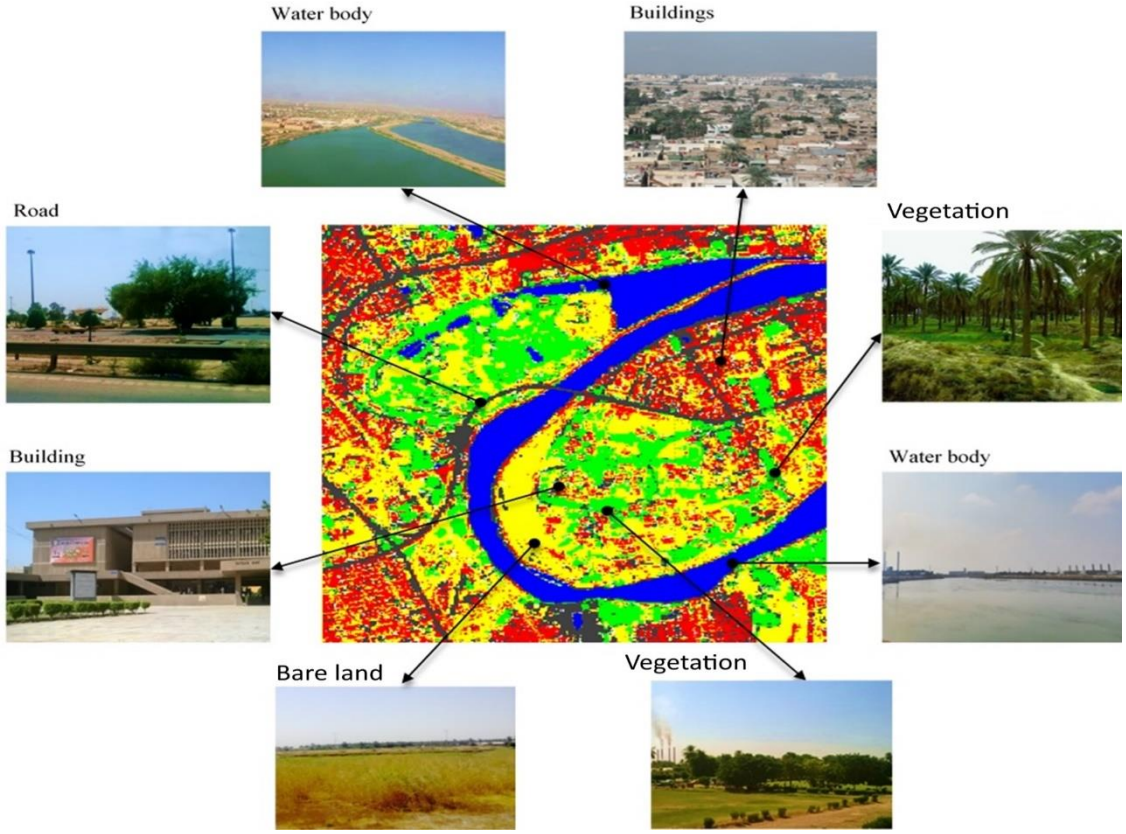

Figure 9. Visual verification of the final thematic map.

5. Conclusion

The analysis of the reported results confirms that the RF algorithm exhibited remarkable precision in classifying the region of interest with an overall accuracy of 83.33%. Conversely,

the MD algorithm recorded the lowest classification accuracy of 63.33%. The thematic map showed that bare lands and buildings emerged as the most prevalent categories, collectively covering a substantial expanse of 11.97 Km^2. Meanwhile, the category of water bodies occupied the smallest area, spanning a mere 2.78 Km^2. These findings bear significant implications for the future development of the study area, potentially informing land-use planning and resource management. The proposed approach promises to yield valuable insights into land cover dynamics in a broader geographical context. To advance this research, the current methodology was recommended in areas characterized by diverse landcover patterns and leveraging alternative sources of satellite imagery to enhance the robustness of the analysis. Moreover, as another avenue for future research, using Google Earth Engine for land cover and land use classification warrants consideration.

Acknowledgments

The authors acknowledge support from the University of Thi-Qar and Al-Iraqia University. The anonymous reviewers' comments in refining this manuscript are also greatly appreciated.

Statements on compliance with ethical standards and standards of research involving animals

This article does not contain any studies involving animals performed by any authors.

Disclosure and conflict of interest

The authors declare that they have no conflicts of interest.

References

[1] P. J. Mitchell, A. L. Downie, and M. Diesing, "How good is my map? A tool for semi-automated thematic mapping and spatially explicit confidence assessment," *Environ. Model. Softw.*, vol. 108, pp. 111–122, 2018, doi: 10.1016/j.envsoft.2018.07.014.

[2] A. Taati, F. Sarmadian, A. Mousavi, C. T. H. Pour, and A. H. E. Shahir, "Land use classification using support vector machine and maximum likelihood algorithms by Landsat 5 TM images," *Walailak J. Sci. Technol.*, vol. 12, no. 8, pp. 681–687, 2015, doi: 10.14456/vol12iss11pp.

[3] H. A. Atiyah, S. M. Khazael, and A. Q. Makhool, "Spatiotemporal Drought Monitoring Using Remote Sensing Technique in Babel-Iraq," *Iraqi J. Sci.*, vol. 64, no. 3, pp. 1535–1544, 2023, doi: 10.24996/IJS.2023.64.3.41.

[4] S. K. Hanoon, A. F. Abdullah, H. Z. M. Shafri, and A. Wayayok, "Using Supervised Classification technique to monitor hydrological systems of Mesopotamia marshes in Dhi-Qar province (Iraq)," *Int. Geosci. Remote Sens. Symp.*, vol. 2022-July, no. July, pp. 6189–6192, 2022, doi: 10.1109/IGARSS46834.2022.9884428.

[5] A. Tzepkenlis, K. Marthoglou, N. G.-R. Sensing, and undefined 2023, "Efficient Deep Semantic Segmentation for Land Cover Classification Using Sentinel Imagery," *mdpi.com*, Accessed: Oct. 22, 2023. [Online]. Available: https://www.mdpi.com/2072-4292/15/8/2027

[6] J. I. Faraj and F. H. Mahmood, "Extraction of Vacant Lands for Baghdad City Using Two Classification Methods of Very High-Resolution Satellite Images," *Iraqi J. Sci.*, vol. 59, no. 4C, pp. 2336–2342, 2018, doi: 10.24996/ijs.2018.59.4C.21.

[7] J. R. Jensen, *Introductory digital image processing: a remote sensing perspective. Second edition*. 1996.

[8] M. A. Moharram and D. M. Sundaram, "Dimensionality reduction strategies for land use land cover classification based on airborne hyperspectral imagery: a survey," *Environ. Sci. Pollut. Res.*, vol. 30, no. 3, pp. 5580–5602, Jan. 2023, doi: 10.1007/S11356-022-24202-2.

[9] S. M. Khazael and M. Al-Bakri, "The Optimum Site Selection for Solar Energy Farms using AHP in GIS Environment, A Case Study of Iraq," *Iraqi J. Sci.*, vol. 62, no. 11, pp. 4571–4587, Dec. 2021, doi: 10.24996/IJS.2021.62.11(SI).36.

[10] B. Rimal, S. Rijal, and R. Kunwar, "Comparing Support Vector Machines and Maximum

Likelihood Classifiers for Mapping of Urbanization," *J. Indian Soc. Remote Sens.*, vol. 48, no. 1, pp. 71–79, Jan. 2020, doi: 10.1007/S12524-019-01056-9/TABLES/4.

[11] Y. Dang, N. Jiang, H. Hu, Z. Ji, and W. Zhang, "Image classification based on quantum K-Nearest-Neighbor algorithm," *Quantum Inf. Process. 2018 179*, vol. 17, no. 9, pp. 1–18, Aug. 2018, doi: 10.1007/S11128-018-2004-9.

[12] L. Breiman, "Random Forests," *Mach. Learn. 2001 451*, vol. 45, no. 1, pp. 5–32, Oct. 2001, doi: 10.1023/A:1010933404324.

[13] R. H. Topaloğlu, E. Sertel, and N. Musaoğlu, "Assessment of classification accuracies of Sentinel-2 and Landsat-8 data for land cover/use mapping," in *International Archives of the Photogrammetry, Remote Sensing and Spatial Information Sciences - ISPRS Archives*, 2016. doi: 10.5194/isprsarchives-XLI-B8-1055-2016.

[14] N. Yusof, H. Z. M. Shafri, and N. S. N. Shaharum, "The use of Landsat-8 and Sentinel-2 imageries in detecting and mapping rubber trees," *J. Rubber Res.*, vol. 24, no. 1, pp. 121–135, 2021, doi: 10.1007/s42464-020-00078-0.

[15] M. A. Ahmed and W. A. Ahmad, "Integration Remote Sensing and GIS Techniques to Evaluate Land Use- Land Cover of Baghdad Region and Nearby Areas," *Iraqi J. Sci.*, vol. 55, no. 1, pp. 184–192, 2014.

[16] B. Q. Al-Abadi, M. S. Mahdi, and Y. C. Bukheet, "Study of Land Cover Changes of Baghdad Using Multi-Temporal Landsat Satellite Images," *Iraqi J. Sci.*, vol. 57, no. 3B, pp. 2146–2160, 2016.

[17] Esi, "SNAP – STEP." https://step.esa.int/main/toolboxes/snap/ (accessed Jun. 17, 2021).

[18] Esri, "About ArcGIS | Mapping & Analytics Software and Services." https://www.esri.com/en-us/arcgis/about-arcgis/overview (accessed Jun. 17, 2021).

[19] J. C. Padró, F. J. Muñoz, L. Á. Ávila, L. Pesquer, and X. Pons, "Radiometric Correction of Landsat-8 and Sentinel-2A Scenes Using Drone Imagery in Synergy with Field Spectroradiometry," *Remote Sens. 2018, Vol. 10, Page 1687*, vol. 10, no. 11, p. 1687, Oct. 2018, doi: 10.3390/RS10111687.

[20] H. Dibs, H. A. Hasab, J. K. Al-Rifaie, and N. Al-Ansari, "An Optimal Approach for Land-Use / Land-Cover Mapping by Integration and Fusion of Multispectral Landsat OLI Images: Case Study in Baghdad, Iraq," *Water. Air. Soil Pollut.*, 2020, doi: 10.1007/s11270-020-04846-x.

[21] A. W. Jacob *et al.*, "Sentinel-1 InSAR Coherence for Land Cover Mapping: A Comparison of Multiple Feature-Based Classifiers," *IEEE J. Sel. Top. Appl. Earth Obs. Remote Sens.*, vol. 13, pp. 535–552, 2020, doi: 10.1109/JSTARS.2019.2958847.

[22] J. R. Otukei and T. Blaschke, "Land cover change assessment using decision trees, support vector machines and maximum likelihood classification algorithms," *Int. J. Appl. Earth Obs. Geoinf.*, vol. 12, pp. S27–S31, 2010, doi: 10.1016/j.jag.2009.11.002.

[23] H. N. Mahendra, S. Mallikarjunaswamy, V. Rekha, V. Puspalatha, and N. Sharmila, "Performance analysis of different classifier for remote sensing application," *Int. J. Eng. Adv. Technol.*, vol. 9, no. 1, 2019, doi: 10.35940/ijeat.A1879.109119.

[24] A. Razafinimaro, A. Richard Hajalalaina, Z. Tantely Reziky, E. Delaitre, and A. Andrianarivo, "Landsat8 Satellite Image Classification with ERDAS for Mapping the Kalambatritra Special Reserve," *Am. J. Remote Sens.*, vol. 9, no. 1, p. 16, 2021, doi: 10.11648/j.ajrs.20210901.12.

[25] H. Franco-Lopez, A. R. Ek, and M. E. Bauer, "Estimation and mapping of forest stand density, volume, and cover type using the k-nearest neighbors method," *Remote Sens. Environ.*, vol. 77, no. 3, 2001, doi: 10.1016/S0034-4257(01)00209-7.

[26] P. Thanh Noi and M. Kappas, "Comparison of Random Forest, k-Nearest Neighbor, and Support Vector Machine Classifiers for Land Cover Classification Using Sentinel-2 Imagery," *Sensors (Basel).*, vol. 18, no. 1, 2017, doi: 10.3390/s18010018.

[27] M. S. Sachit, H. Z. M. Shafri, A. F. Abdullah, A. S. M. Rafie, and M. B. A. Gibril, "Global Spatial Suitability Mapping of Wind and Solar Systems Using an Explainable AI-Based Approach," *ISPRS Int. J. Geo-Information*, vol. 11, no. 8, 2022, doi: 10.3390/ijgi11080422.

[28] A. Wasniewski, A. Hoscilo, B. Zagajewski, and D. Moukétou-Tarazewicz, "Assessment of sentinel-2 satellite images and random forest classifier for rainforest mapping in Gabon," *Forests*, vol. 11, no. 9, 2020, doi: 10.3390/f11090941.